Acidizing Process in Acid Fracturing

B.E. Bekbauov

Al-Farabi Kazakh National University, Faculty of Mechanics and Mathematics
39/47 Masanchi str., 050012, Almaty, Republic of Kazakhstan

Abstract

The theory and numerical implementation of acid-fracturing model that solves the 2D fracture geometry leakoff, acid transport and acid-rock reaction simultaneously will be presented. The mathematical model provides a penetration distance for acid fracturing. Due to limitation of analytical solution, a finite-difference method was developed for modelling the fracture acidizing process. Example was solved for HCl reaction in limestone and dolomite fractures, and the results are presented in graphical form. The acid-transport model integrates a number of features which were not accounted for an earlier design models: comprehensive study of hydrodynamic process; acidizing controlled by mass transfer, rate of reaction, and leakoff. Coupling with reservoir forecasting models gives the ability to optimize the job.

Nomenclature

Symbol	Explanation	Unit
A	elemental area	L^2
b	fracture width (width between parallel plates, $b = 2b_{l/2}$)	L
C	acid concentration	m/V
D_e	effective diffusion coefficient	L^2/t
k	acid-rock reaction rate coefficient	L/t
q	Rate	V/t
t	Time	sec
v_l	leak-off velocity	L/t
u, v	flow velocity components	L/t
μ	fluid viscosity	cp
v	Kinematic viscosity of fluid, $\nu = \mu/\rho$	L^2/t
ρ	Density	m/V
ϕ	Porosity	
x,y	length and width coordinates	L
Ca	acid concentration at $y=0$	%
Cb	Boundary concentration	%
Cav	width-averaged acid concentration	%
Lxa	acid penetration distance along the axis of symmetry	L
Lxb	acid penetration distance along the boundary of fracture	L
Q_{al}	the amount of acid lost to the formation by leakoff	L^2/t
Q_{ar}	reacted amount of acid	L^2/t
Q_{at}	total loss of acid by leakoff and reaction	L^2/t
A	Acid	
B	boundary (fracture wall)	
e	Effective	
eq	Equilibrium	
i	Injection	
l	Leakoff (loss)	
t	Total	
m	Reaction order	
$n(n+1)$	Beginning and end of time step	

*corresponding author. E-mail: Bakhbergen.Bekbauov@kaznu.kz

Introduction

Acids are widely used in the hydraulic fracturing of reservoirs to stimulate wells. The purpose of the acid is to selectively react with and dissolve portions of the fracture wall so that a finite fluid conductivity remains when the well is returned to production.

Acid fracturing is currently receiving renewed attention as a well stimulation technique. During a period of intense study in the 1970's, the basic understanding of the reaction kinetics and acid transport in the acid-fracturing process was established experimentally and theoretically [1-3]. Very little work on acid-fracturing design was reported in the 1980's. Ben Naceur and Economides [4] and Lo and Dean [5] presented improved models of acid transport,

© 2009 al-Farabi Kazakh National University Printed in Kazakhstan

coupled with a specific 2D model of fracture geometry. Gdanski and Lee [6] described a more general model, but their work lacked mathematical details. Settari A. [7] neglected diffusion along the fracture, and used a simplified hydrodynamic model.

One important variable that must be known in designing these treatments is the distance in which acid will penetrate through the fracture before being completely spent. This distance is usually called the acid penetration length and is an essential part of the information needed for predicting productivity after acidizing [8, 9]. Because of its importance in predicting stimulation ratios, acid penetration into a fracture has been studied by several investigators [10-14].

This paper gives the theory of a comprehensive acid-fracturing model, the numerical implementation of the acid-transport and leakoff solution, and examples illustrating various features of the model. The model includes a number of new features essential for modern design: comprehensive study of hydrodynamic process in acid fracturing treatments; acidizing process controlled by both mass transfer and rate of reaction.

This formulation is considerably more general than the model described in Ref. 5, which assumes infinite reaction rate. These features are illustrated by examples of acid transport under different physical conditions (limited by mass transfer, reaction rate, effect of reaction order, etc.).

We present here the results of an investigation of the use of a mathematical model for predicting acid spending in a fracture.

Mathematical Model for Acid Fracturing

A mathematical model is developed that yields the distance to which live acid may penetrate into a fracture. Navier-Stokes equation was used to model the flow within a fracture of unit height:

$$\frac{\partial u}{\partial t}+u\frac{\partial u}{\partial x}+v\frac{\partial u}{\partial y}=-\frac{1}{\rho}\frac{\partial p}{\partial x}+\nu\left(\frac{\partial^2 u}{\partial x^2}+\frac{\partial^2 u}{\partial y^2}\right)$$
$$\frac{\partial v}{\partial t}+u\frac{\partial v}{\partial x}+v\frac{\partial v}{\partial y}=-\frac{1}{\rho}\frac{\partial p}{\partial y}+\nu\left(\frac{\partial^2 v}{\partial x^2}+\frac{\partial^2 v}{\partial y^2}\right) \quad (1)$$

$$\frac{\partial u}{\partial x}+\frac{\partial v}{\partial y}=0 \quad (2)$$

Here the acid leakoff velocity, v_l, is assumed constant over the fracture length. Williams and Nierode have noted that this assumption is probably reasonable for the first 80 percent of fracture length. The model can be modified further if a varying leakoff rate is found to be important. We assume that before acidizing inside the fracture the pressures are the back pressure. When acidizing begins, acid is introduced into the fracture with a constant injection rate from the inlet side at $x=0$. Leakoff velocity is given at the top boundary where $y=h$. There is no flow at axis of symmetry where $y=0$. At the outlet side where $x=L$, the pressure is the back pressure. Chorin's projection method was applied to solve Navier-Stokes equation. The successive over-relaxation method was used for the numerical solution of the pressure Poisson's equation. The methods and boundary conditions for Navier-Stokes equation were discussed in [15, 16].

An equation that will yield the acid concentration as it flows down the fracture may be obtained by a material balance as

$$\frac{\partial C}{\partial t}+\vec{V}\cdot gradC=div\left(D_e gradC\right) \quad (3)$$

Eq. 3 must be solved subject to the boundary conditions

$$C(x,y)=0 \text{ at } t=0, \quad (3a)$$
$$C=C_i \quad \text{at } x=0,\ t>0, \quad (3b)$$
$$\frac{\partial C}{\partial y}=0 \quad \text{at } y=0, \quad (3c)$$
$$\frac{\partial C}{\partial x}=0 \quad \text{at } x=L. \quad (3d)$$

We assume that before acidizing, inside the fracture the acid concentration is zero. When acidizing begins, acid is introduced into the fracture with a constant injection rate from the inlet side at $x=0$. The acid concentration at the inlet side is C_i.

The boundary condition that allows for both finite and infinitely fast reaction at the fracture wall is [1, 7]

$$-D_e\left(\partial C/\partial y\right)\big|_{y=b/2}=k\left(1-\phi\right)\left(C_B-C_{eq}\right)^m. \quad (3e)$$

Eqs. 1, 2, and 3 are used for computer simulation with proper boundary conditions. Eqs. 3a – 3e represent the initial and boundary conditions for our numerical model.

The total loss of acid by reaction and leakoff is

$$q_{At}=k\left(1-\phi\right)\left(C_B-C_{eq}\right)^m+v_l C_l \ . \quad (4)$$

The model of acid fracturing is presented in Fig. 1. For simplicity, an element of a fracture with constant width is considered. The injection rate and fracture width remain constant throughout the test. Actually the fracture width changes throughout the experiment. The numerical model was verified against the numerical solutions of Roberts and Guin. To match them, the model was run with a constant fracture width. We think that the constant fracture width and leakoff make the interpretation easier compared to the model coupled with a fracture simulator. The modelling of a variable width fractures have been scheduled for implementation in the future.

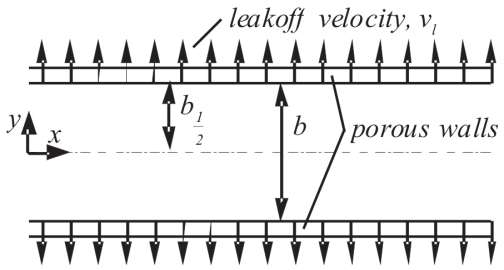

Fig. 1. Model of fracture

Results and Discussion

The mass conservation properties of the numerical method are shown in Table 1.

Table 1
Treatment data for field example and the mass conservation properties of the numerical method

	Inlet Velocity, U_i, [m/sec	Leakoff Velocity, v_l, [m/sec]	Cross Section, x, [M]	Rate, Q, [m^2/sec]
Case 1	$4.016 \cdot 10^{-4}$	$2 \cdot 10^{-6}$	0	2.008E -6
			0.5	2.0076E -6
			1	2.0074E -6
Case 2	$5 \cdot 10^{-3}$	$2.5 \cdot 10^{-6}$	0	2.5 E -5
			1	2.4996E -5
			2	2.4994E -5

Primitive variable approach is compared with the streamfunction-vorticity method. The results of the calculations for streamfunction-vorticity formulation of the Navier-Stokes equations are presented in Figs 2a and 2b.

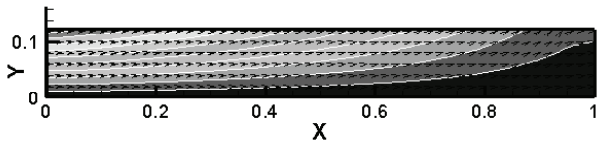

a)

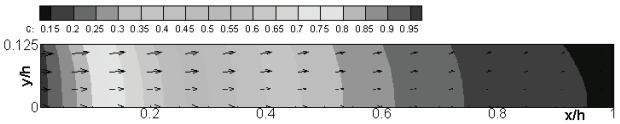

b)

Fig. 2. Calculation results for the vorticity-streamfunction formulation: velocity field and streamlines; b) velocity field and acid concentration distribution.

As an example, we consider treating a formation with properties given in Table 2, which corresponds to Case 2.

Table 2
Reservoir data for the field example

Parameter	Symbol, unit	Value
Fracture Half Width	H, [m]	$5 \cdot 10^{-3}$
Fracture Length	L, [m]	2
Porosity	ϕ	0.15
Average Reservoir Pressure	p_{av}, [Pa]	$23 \cdot 10^{6}$
Fluid Density	ϕ, [kg/m^3]	1000
Fluid Viscosity	μ, [cp]	0.72
Inlet Concentration	C_i, [%]	28

To illustrate the various aspects of the physics, four case studies were carried out with Lo and Dean's [5] and Settari's [7] data. Table 3 shows the common data. Because the model of Ref. 5 assumes an infinite rate of reaction and C_B=0, a high value of reaction constant, k=0.1 *cm/sec,* m=1 and C_{eq}=0 are used here to test the model. Because Ref. 5 used a constant value of D_e=0.0001 cm^2/sec, the corresponding solution with this value is also shown.

To test other features (Ref. 7), the same basic set of data was used with modifications. The use of a more reasonable value for the reaction constant, k=0.1 *cm/sec*, results in higher boundary concentration and demonstrates that the formulation of the model can handle acidizing controlled by mass transfer, reaction rate, of a combination of both.

The use of nonzero C_{eq} results in unspent acid. This may be important for treatments with weak acids or low concentration acid treatment, and takes into account the effect of reverse reaction (Case C. in Table 3). Examples of treatment design illustrate these features. Results are presented in graphical form such as shown in Figs 3-6.

Having a reaction order lower than 1 increases the rate of reaction. This makes the result for k=0.01 and m=0.5 look more like the infinite-reacting system. The feature is important because the measurements often show low values of m.

The effects of reaction order m, reaction rate coefficient k, effective diffusion coefficient D_e, and equilibrium concentration C_{eq} on acid penetration distance (defined as the distance the live acid would travel before its concentration is spent to) are examined, and the results are shown in Figs. 4 – A, B, C, D for axis symmetry line and boundary line concentrations.

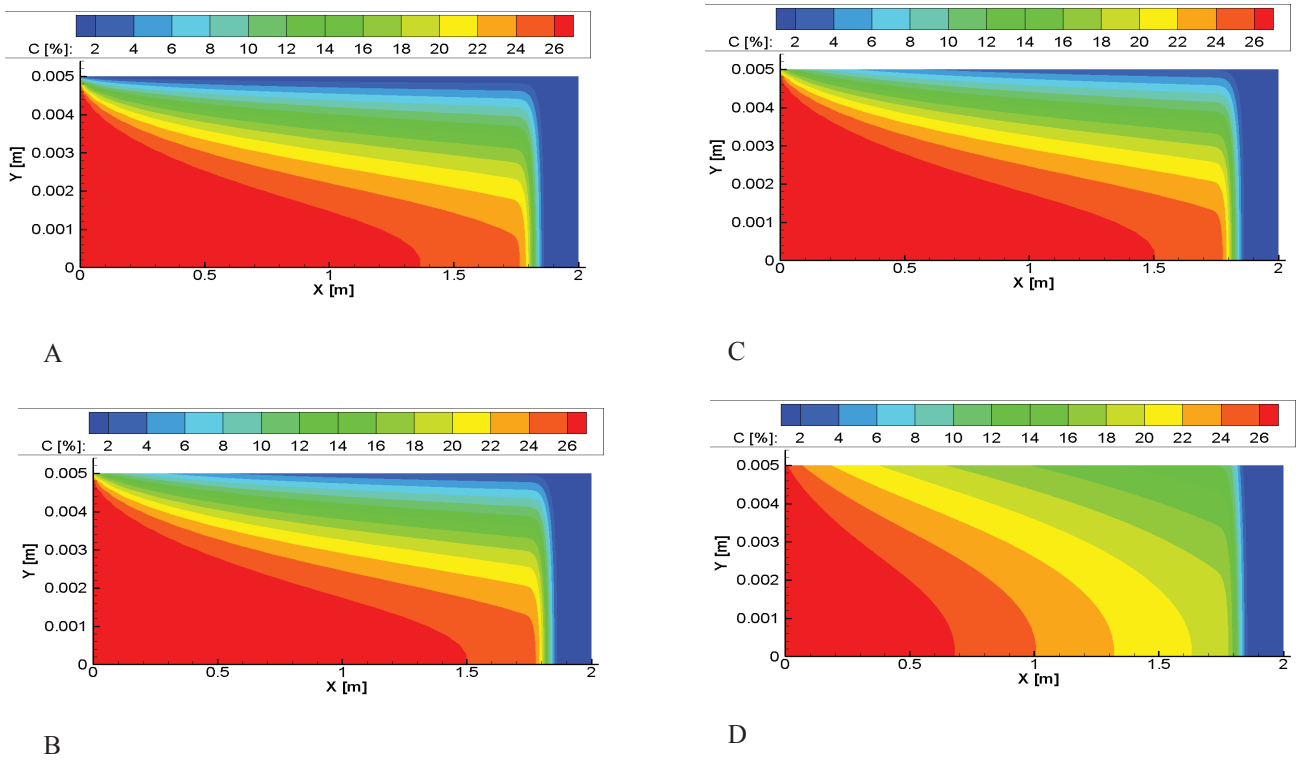

Fig. 3. Acid concentration field in fracture.

Table 3

Acid-transport test data

Parameter	Symbol, unit	Cases considered			
		A.	B.	C.	D.
Reaction Order	m	1	0.5	0.5	0.441
Reaction Rate Coefficient	k [m/sec]	10^{-3}	10^{-4}	10^{-4}	$5 \cdot 10^{-5}$
Effective Diffusion Coefficient	D_e [m^2/sec]	10^{-8}	10^{-8}	10^{-8}	$4.3 \cdot 10^{-8}$
Equilibrium Concentration	C_{eq} [%]	0	0	0.2	0

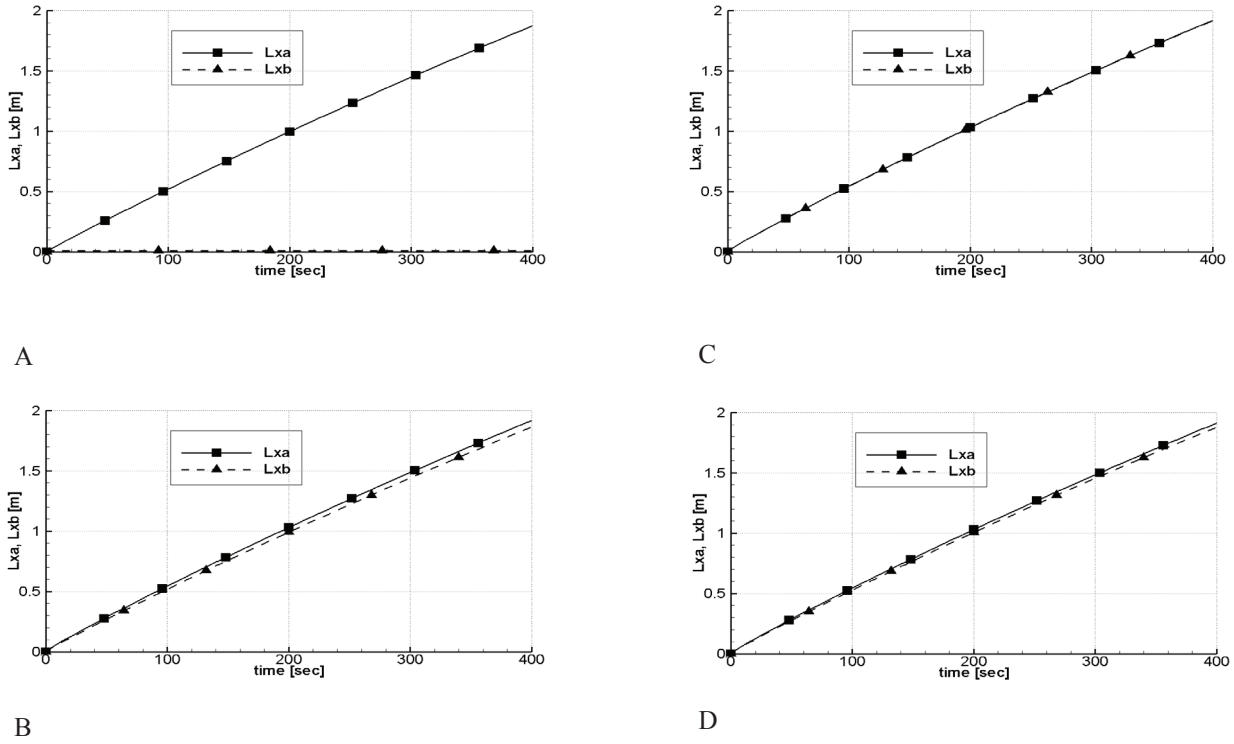

Fig. 4. Acid penetration distance vs. time.

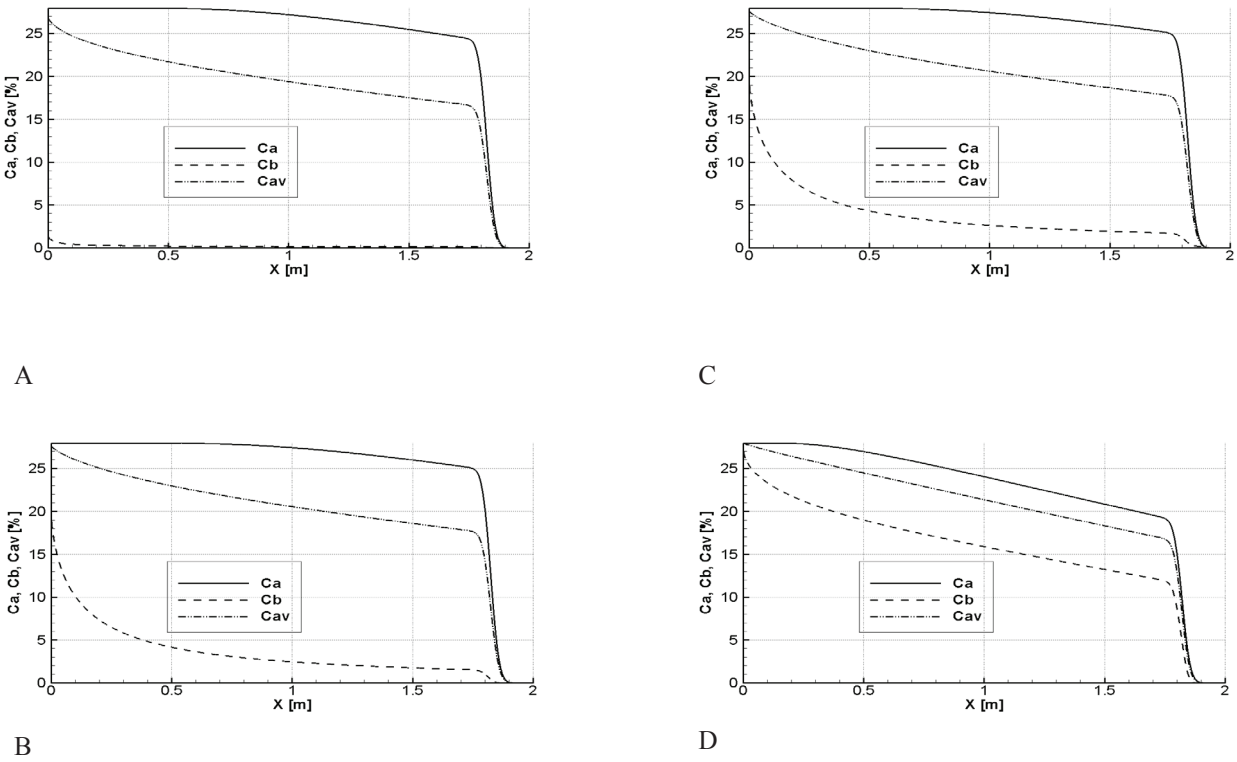

Fig. 5. Concentration profiles.

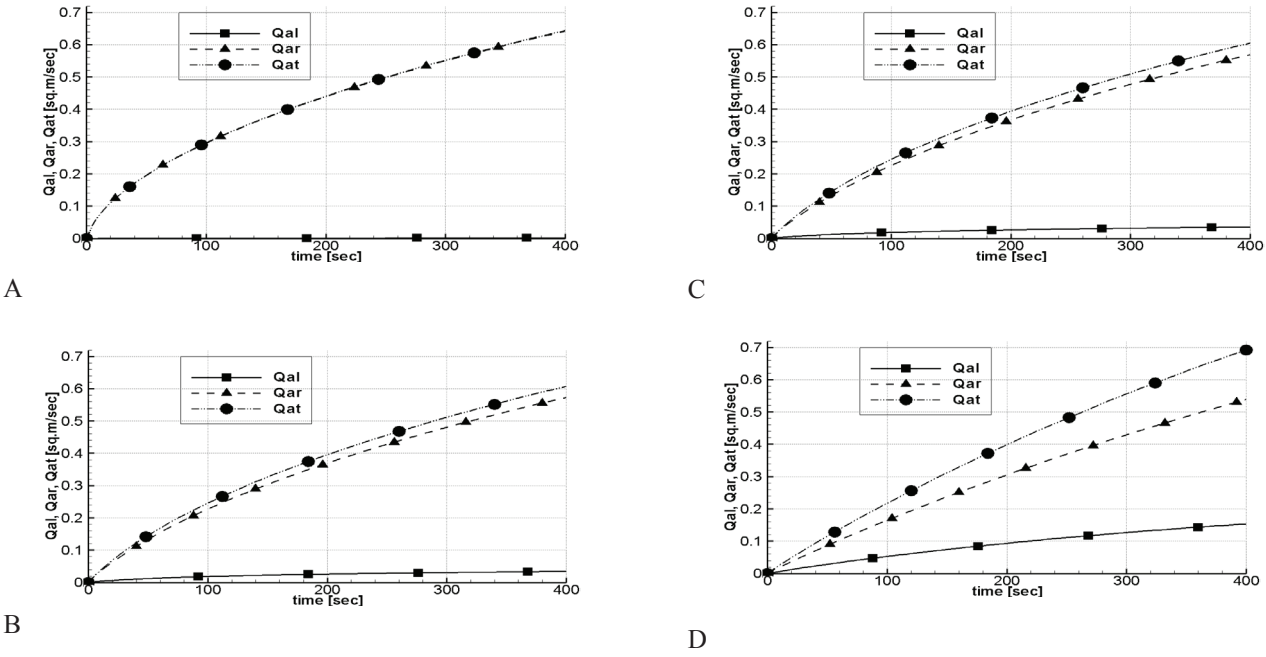

Fig. 6. The amount of acid lost to the formation by leakoff, reacted amount by reaction and the total loss.

The effects of the same parameters on acid concentration distribution are shown in Figs. 5 – A, B, C and D for the Case 2 in Table 1. Three curves for , and are shown in each figure. The curves represent acid concentration at axis of symmetry, boundary concentration, and width-averaged acid concentration, respectively.

Figs. 6 – A, B, C and D show the effect of on penetration length is more significant than effects of other parameters: the higher the effective mixing coefficient, the more intensive acid lost by reaction and, consequently, the shorter the penetration length.

To test other features, the same acid transport test data in Table 3 was used. After the numerical test for continuity (Table 1), more realistic example shows the effect of each parameter in Table 3. As an example, we consider treating a formation with properties given in Table 4.

For the final, more realistic example the reaction data were k=0.005, m=0.441, D_e=0.00043 cm^2/sec, and C_{eq}=0. The result is a significant decrease in fracture penetration (Fig. 7-D).

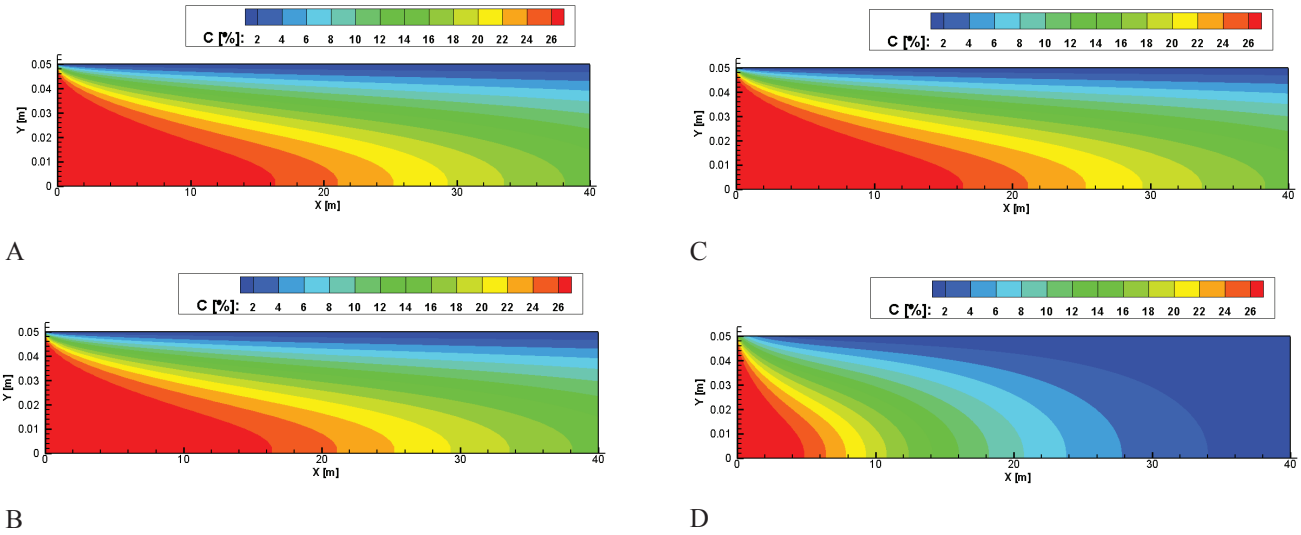

Fig. 7. Acid concentration field in fracture for cases A, B, C and D respectively at t=23.4417 h.

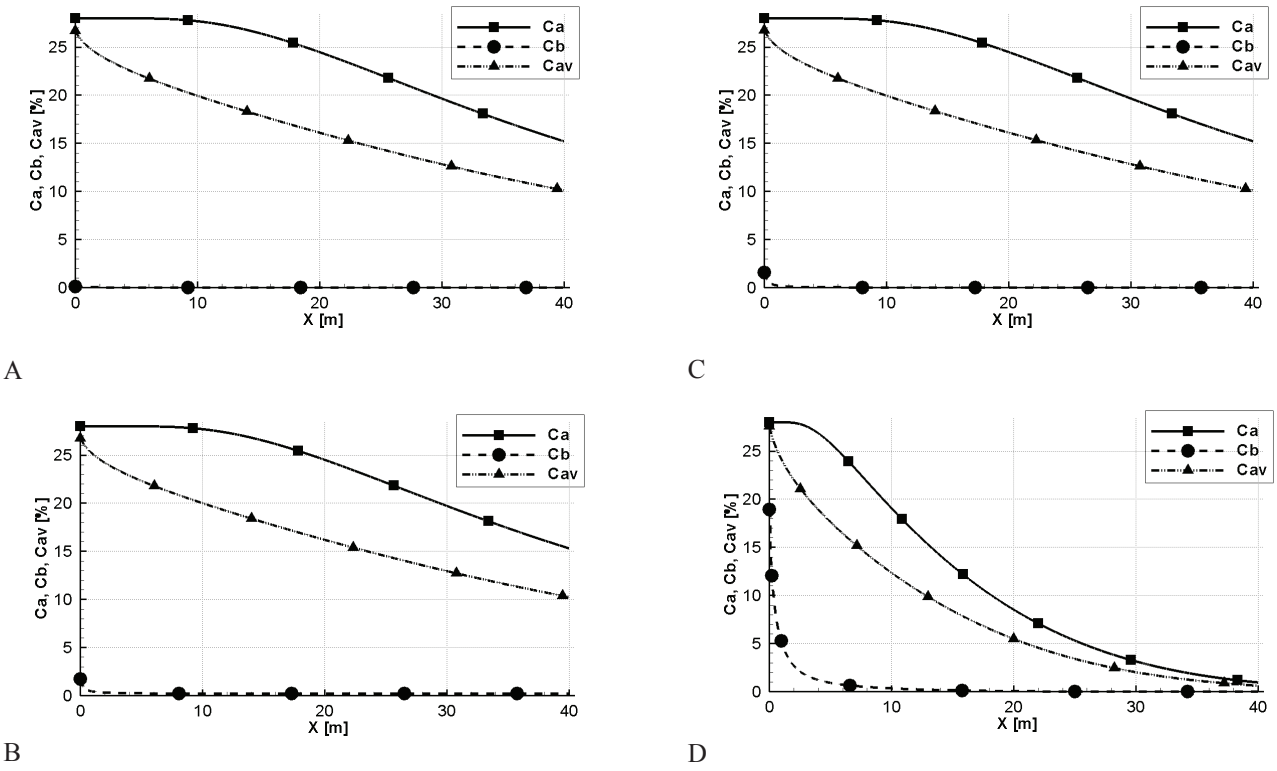

Fig. 8. Concentration profiles for cases A, B, C and D respectively at t=23.4417 h.

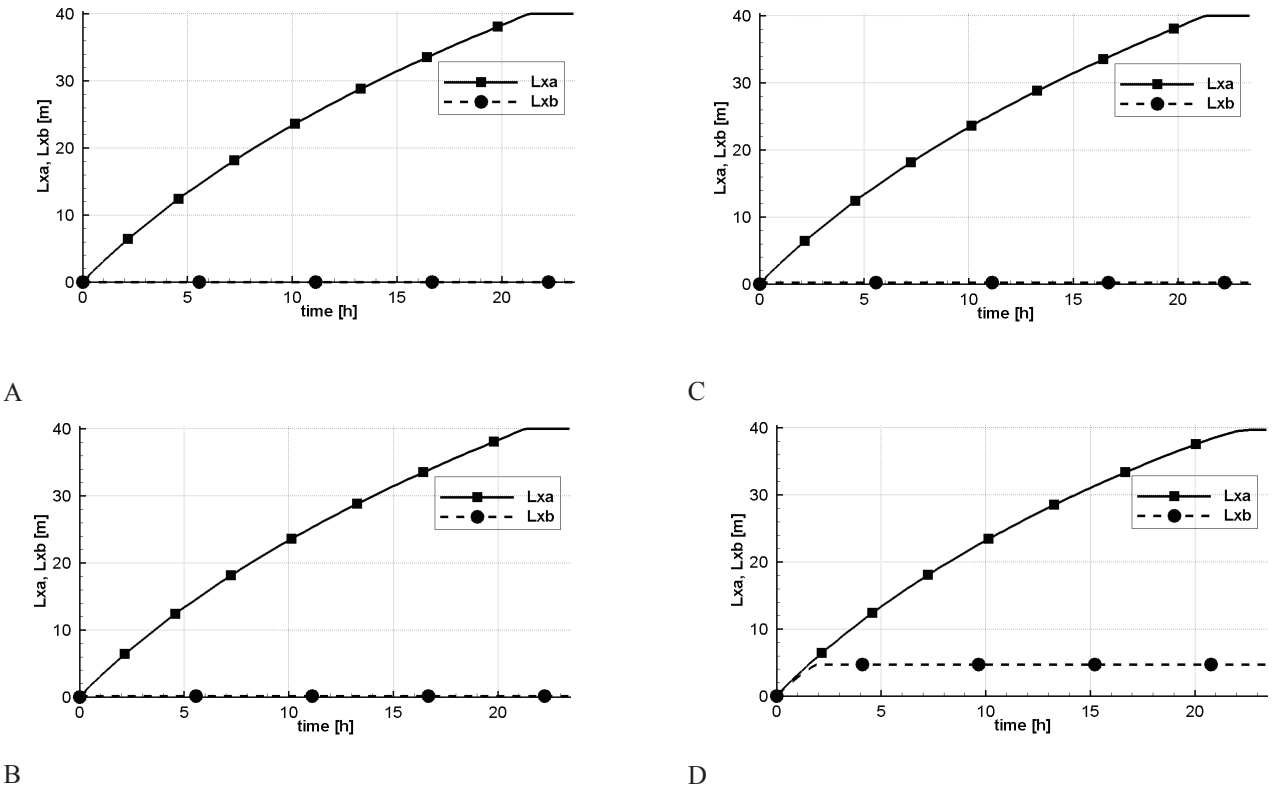

Fig. 9. Acid penetration distance for cases A, B, C and D respectively.

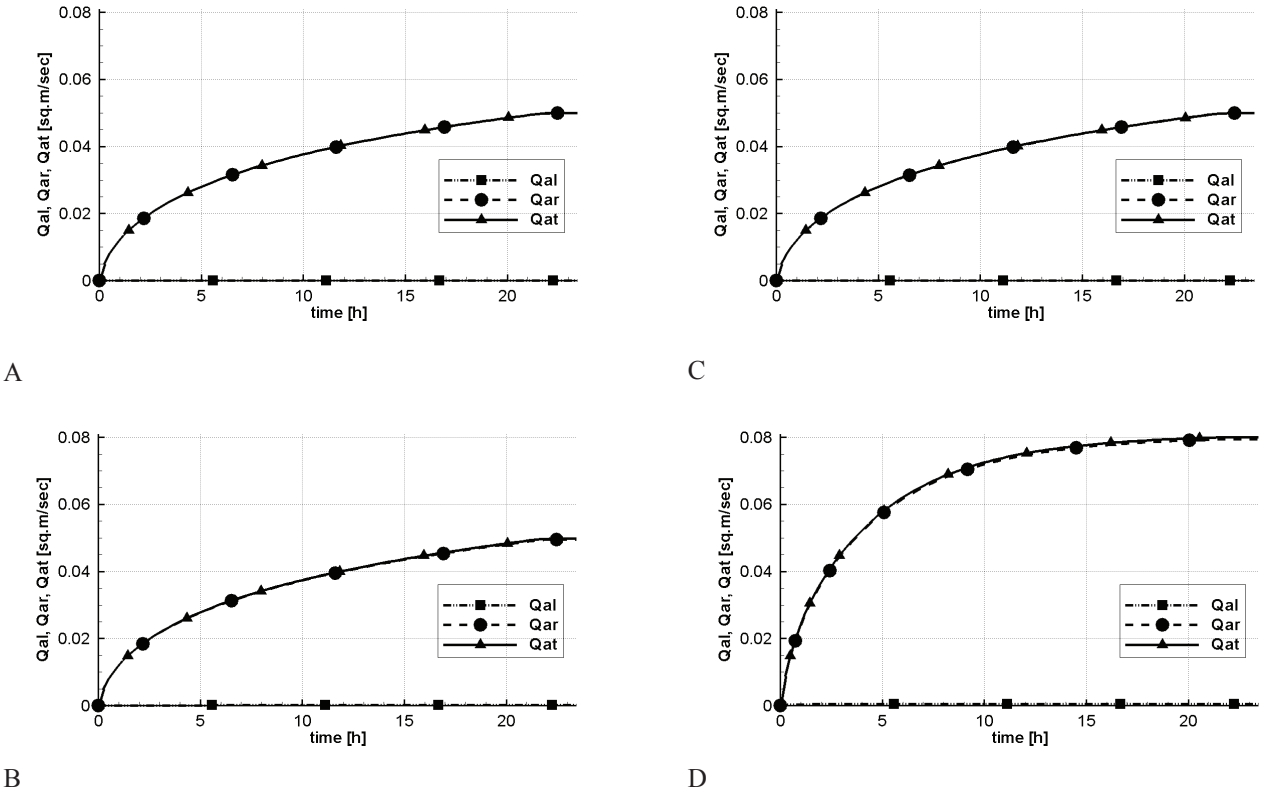

Fig. 10. The amount of acid lost to the formation by leakoff, reacted amount by reaction and the total loss.

The example show how the model can be used to determine the sensitivity of acid penetration to various parameters. The above parameters, except for the effective diffusion coefficient, although changing the acid concentration profile, do not have a large effect on penetration. The increase in effective diffusion coefficient can cause the penetration distance to decrease significantly, as shown below (Figs 7-10). Figures 7 and 8 show the resulting acid distribution profiles. Figure 9 shows acid penetration speed along the axis of symmetry and boundary of fracture. Figure 10 shows the amount of acid lost to the formation by leakoff, reacted amount by reaction and the total loss.

Conclusion

A mathematical model has been presented for describing acid spending in a fracture when the over-all rate of spending is affected by the surface reaction rate and the leakoff. A method to characterize the leakoff and the reaction in acid jobs is developed. The model is solved by numerical method and results are given in graphical form for design purposes.

A comprehensive study of hydrodynamic process in acid fracturing treatments was carried out. While the complete comparison of these algorithms is not yet accomplished, our results indicate that for those flows in which the surface can be approximated as a fixed level surface, the streamfunction-vorticity form can produce results equivalent to the primitive variable form. However, quantitative and qualitative comparisons of the primitive variables method's solutions with the streamfunction-vorticity computations show that the primitive variable numerical approach is robust and yields a more accurate solution due to its implementation of the flow boundary conditions.

The acidizing process can be controlled by mass transfer, leakoff, rate of reaction and allows arbitrary order of reaction and equilibrium concentration. Effect of surface reaction rate constant, reaction order, and the effective mixing coefficient was considered to account for the effect of the surface reaction rate on the spending of HCl in a dolomite fracture.

Future model extensions will include:

- 3D Navier-Stokes;
- Domain is growing with time.

References

1. Roberts, L.D. and Guin, J.A.: "The Effect of Surface Kinetics in Fracture Acidizing," SPEJ (August, 1974) 385-95; Trans., AIME, 257.
2. Williams, B.B. et al.: "Characterization of Liquid-Solid Reactions. Hydrochloric Acid-Calcium Carbonate Reaction," Ind. & Eng. Chem. Fund. (1970) 9, No. 4, 589.
3. Nierode, D.E. and Williams, B.B.: "Characteristics of Acid Reaction in Limestone Formations," SPEJ (Dec. 1971) 406-18; Trans., AIME, 251.
4. Ben Naceur, K. and Economides, M.J.: "Design and Evaluation of Acid Fracturing Treatments," paper SPE 18978 presented at the 1989 SPE Rocky Mountain Regional/Low Permeability Reservoirs Symposium, Denver, March 6-8.
5. Lo, K.K. and Dean, R.H.: "Modeling of Acid Fracturing," SPEPE (May 1989) 194-200; Trans., AIME, 287.
6. Gdanski, R.D. and Lee, W.S.: "On the Design of Fracture Acidizing Treatments," paper SPE 18885 presented at the 1989 SPE Production Operations Symposium, Oklahoma City, March 13-14.
7. Settari A., Simtech Consulting Services Ltd. "Modeling of Acid-Fracturing Treatments," SPE Production & Facilities, Volume 8, Number 1, February 1993.
8. Tinsley, J. M., Williams, J. R., Tiner, R. L., and Malone, W. T.: "Vertical Fracture Height – Its Effect on Steady-State Production Increase," J. Pet. Tech. (May 1969) 633-638; Trans., AIME, Vol. 246.
9. McCuire, W. J., and Sikora, V. J.: "The Effect of Vertical Fractures on Well Productivity," Trans., AIME (1960) Vol. 219, 401-403.
10. Dill, W. R.: "Reaction Times of Hydrochloric Acetic Acid Solutions on Limestone," paper presented at 16th Southwest Regional ACS Meeting, Oklahoma City, Okla (Dec. 1960).
11. Barron, A. N., Hendrickson, A. R., and Wieland, D. R.: "The Effect of Flow on Acid Reactivity in a Carbonate Fracture," J. Pet. Tech. (April 1962) 409-415; Trans., AIME, Vol. 225.
12. Williams, B. B., Gidley, J. L., Guin, J. A., and Schechter, R. S.: "Characterization of Liquid-Solid Reactions," Ind. And Eng. Chem. Fund. (1970) Vol. 9, 589.
13. Nierode, D. E., and Williams, B. B.: "Characteristics of Acid Reaction in Limestone Formations," Soc. Pet. Eng. J. (Dec 1971) 406-418; Trans., AIME, Vol. 251.
14. Williams, B. B., and Nierode, D. E.: "Design of Acid Fracturing Treatments," J. Pet. Tech. (July 1972) 849-859; Trans., AIME, Vol. 253.
15. Belocerkovsky, O. M.: "Numerical Modelling in Continuum Mechanics," M.: Nauka. Main editorial staff of physical-mathematical literature, 1984. – 520 p.
16. Roache, P.J.: "Computational Fluid Dynamics," Hermosa Publishers, 1976. – 487 p.

Received 19 november 2009.